Letter

Geometrical patterning of receptor sites controls kinetics via many-body effects in bivalent systems

Richard E. Spinney [1,2] Lawrence Lee [2,3] and Richard G. Morris [1,2]

[1]*School of Physics, University of New South Wales, Sydney 2052, Australia*

[2]*EMBL-Australia node in Single Molecule Science, School of Biomedical Sciences, University of New South Wales, Sydney 2052, Australia*

[3]*ARC Centre of Excellence in Synthetic Biology, University of New South Wales, Sydney 2052, Australia*

(Received 31 March 2022; accepted 11 October 2022; published 14 November 2022)

We report on the geometrical patterning of receptor sites in bi- and multi-valent systems as a modality for controlling kinetic behaviors, in both synthetic and biological contexts, that is independent of the underlying chemistry. Exploring motifs, chains, and lattices of receptor sites, we recast this phenomenon as one of many-body coordination, making contact with classical treatments of interacting systems, implicating geometric frustration as an important heuristic for rational design. In doing so, we also reveal the possibility of other tunable spatio-temporal features, such as correlation lengths, mean-squared displacements, and percolation-like transitions.

DOI: 10.1103/PhysRevResearch.4.L042028

Multivalency underpins several important functions in cell and molecular biology. It simultaneously confers an effective increase in binding affinity [1–6], so-called *avidity*, whilst also facilitating concentration-dependent destabilization and turnover [7–10], typically referred to as *competitive exchange* [Fig. 1(a)]. These dual mechanisms, alongside the enhancement of competitive exchange due to neighboring receptor sites—coined *multi-site* competitive exchange [11] [Fig. 1(b)]—underpin a wide variety of diverse phenomena across a range of scales, including toe-hold exchange [7] in DNA hybridization, liquid-liquid de-mixing [12] and receptor-ligand clustering [13] in sub-cellular aggregates, and specificity [14] in the adaptive immune response of T-cells.

Multivalency is also of significant interest to a range of synthetic systems, including: *de novo* proteins [15,16]; nanoparticles, micelles, membranes and other supra molecular biological assemblies [17]; colloidal soft matter [18–20], and; novel materials, such as vitrimers [21,22]. However, spatial control over binding sites—e.g., the patterning of ligands or other surface chemistry in either biological assemblies [17] or "patchy" colloids [23,24]—has been a recurring challenge for engineering emergent spatio-temporal behaviors in such systems, as well as reproducing and/or leveraging the full suite of multivalent behaviors, seen in biology.

In a recent paper [25], the precision of DNA-origami has been shown to address this issue, permitting the construction of entities and complementary substrates whose binding sites each have a geometry, affinity, and specificity that can be specified independently. It is in this light that we now report on parallels between multivalency and many-body interacting systems that have otherwise been overlooked. Specifically, we demonstrate that the *geometrical patterning* of individual receptor sites is tantamount to a qualitatively new design modality, where kinetics (and other emergent behaviors) can be controlled via many-body coordination, independently of the underlying binding affinities.

To show this, we first characterize the varied behaviors associated with motifs of receptor sites that have "all-to-all" symmetry. We are then led to introduce extended, translationally invariant chains and lattices of receptor sites, for which transfer matrices and cavity-like approximations can be brought to bear. Ultimately, these classical many-body techniques permit us to distill core principles for the rational design of kinetics via receptor site geometry. They also reveal other tunable spatio-temporal features, such as correlation lengths, mean-squared displacements, and percolation-like transitions. Our findings prompt us to revisit biological systems and speculate on the role of multivalency in large supra-molecular complexes.

Receptor site geometry as a design modality. We start with a generic bivalent entity, either synthetic nano-baton, protein, or other molecule, whose binding interfaces are each exclusive and complementary to one of two types of receptor site. We call these receptor sites "primary" and "secondary" following [11], and use the term "baton" throughout [Fig. 1(c)]. In this context, the rate of associations of an unbound baton to individual vacant primary and secondary sites can be written as $C_0 k_1^{\mathrm{on}}$ and $C_0 k_2^{\mathrm{on}}$, respectively, where the bulk concentration of batons is given by C_0, and $k_{1/2}^{\mathrm{on}}$ are association rates per mole [Fig. 1(d)]. Batons disassociate from these sites with rates $k_{1/2}^{\mathrm{off}}$, independently of whether the baton is singly or doubly bound, giving site dissociation constants $K_{1/2}$. The rates of association of the unbound ends of singly bound batons are $C_{\mathrm{eff}} k_1^{\mathrm{on}}$ and $C_{\mathrm{eff}} k_2^{\mathrm{on}}$, where C_{eff} represents the large *effective* concentration [1,26,27] that arises from the close proximity between receptor sites and unbound baton ends.

A central quantity of interest is the mean dissociation rate of a bound baton, denoted Γ_{off} (Supplemental Material, Secs. 1 and 2 [28]). In all practical scenarios, Γ_{off} is a

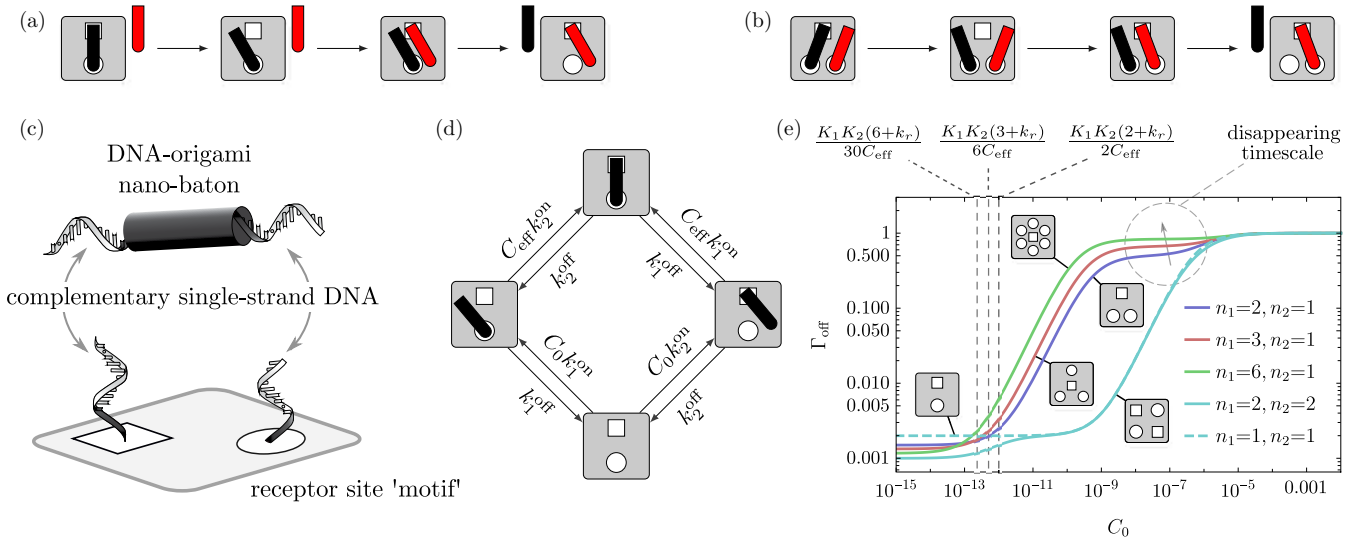

FIG. 1. Competitive exchange involves a bivalent baton from the bulk (red) occupying a receptor site vacated by an attached baton (black), thus destabilizing it (panel a). The effect is amplified when singly bound batons at neighboring sites confer an *effective* concentration that is higher than that of batons in the bulk (panel b). Engineered nanoscale batons which selectively bind to single DNA strands on a DNA origami platform allow arrangements of "primary" (circle) and "secondary" (square) sites into motifs (panel c and [25]). A four-state system comprising a single baton, primary, and secondary receptor site defines the principal kinetic parameters. Mean dissociation rates (per baton) vs. bulk concentration C_0 display two qualitative trends (panel e). Vertical dashed lines indicate the characteristic concentration for motifs $n_1 = 2, 3, 6$, $n_2 = 1$ ($C_0^{\rm char}$ main text). Parameters used throughout: $K_2 = K_1 = 10^{-9}$M, $C_{\rm eff} = 10^{-6}$M, $k_1^{\rm on} = k_2^{\rm on} = 10^9 {\rm M}^{-1}s^{-1}$, informed by [25].

monotonic function of the bulk concentration, C_0. As $C_0 \to 0$ (depletion), $\Gamma_{\rm off}$ is minimized, and captures "bare" avidity—i.e., stability due to multiple receptor sites with no competitive exchange. As $C_0 \to \infty$ (saturation), $\Gamma_{\rm off}$ is maximized, since batons can only bind via one receptor site, and are thus characterised by the nascent dissociation rates of the primary and secondary sites. Between these two limits, the nontrivial dependence of $\Gamma_{\rm off}$ on C_0 is dictated by the geometric arrangement of the receptor sites, which controls the interplay between avidity, competitive exchange, and multi-site effects. Consequently, receptor site geometry can be thought of as a configurable design modality that is independent of the chemical or structural properties of the individual receptor sites themselves.

All-to-all motifs. Consider motifs with *all-to-all* symmetry, where any pair of primary and secondary sites can be simultaneously bound to a single baton. Each motif is therefore uniquely characterized by the number of primary and secondary sites, n_1 and n_2. For a rigid baton, this requires that the distances between all primary and secondary sites are equal; however, this restriction could be plausibly relaxed for flexible molecules and/or synthetic linkers.

Notably, a generic expression for the stationary distribution over baton occupancies can be calculated that encompasses all such motifs, from which $\Gamma_{\rm off}$ follows (Supplemental Material, Sec. 3 [28]) in terms of special functions [29,30]. Despite the complicated generic form, a heuristic appreciation of $\Gamma_{\rm off}$ can be obtained from one of only two general cases, outlined in detail in the Supplemental Material, Sec. 5 [28].

The first case concerns motifs that are one-to-many—*e.g.*, $n_1 > 1$, $n_2 = 1$ [Fig. 1(e)]. Here, as C_0 increases, neighboring sites are increasingly occupied, which facilitates competitive displacement, increasing $\Gamma_{\rm off}$. The onset of this "multi-site exchange" [Fig. 1(b)] depends on the number of neighboring sites (of opposite type) in the motif. We may identify a characteristic concentration for such an onset [Supplemental Material, Sec. 5 [28] and Fig. 1(e)] given as $C_0^{\rm char} \sim K_1 K_2 (k_r + n_1)/C_{\rm eff}(n_1 - 1)n_1 + \mathcal{O}(\varepsilon^2)$, where $K_i = k_i^{\rm off}/k_i^{\rm on}$ are site-specific equilibrium dissociation constants, $k_r = k_2^{\rm on}/k_1^{\rm on}$, given $\varepsilon = K_1/C_{\rm eff} \ll 1$. On further increases in C_0, the multi-site effect plateaus once neighboring sites are reliably occupied, before giving way to bulk competitive exchange in the traditional sense [Fig. 1(a)], as C_0 approaches (and exceeds) $C_{\rm eff}$. This secondary stable timescale vanishes for motifs with increasing numbers of neighbors.

The second case involves equal site numbers, such that $n_1 = n_2$ [Fig. 1(e)]. Here, multi-site effects are effectively eliminated: all partially bound molecules have a complementary site to which they can become doubly bound. As such, the significant increase in $\Gamma_{\rm off}$ occurs due to regular competitive exchange from the bulk, whilst a modest increase for all $n_1 = n_2 > 1$ exists at low concentrations [rising from a rate of $\sim$0.001 to $\sim$0.002 in Fig. 1(e)], which manifests from the removal of vacant neighboring sites by doubly bound batons, decreasing baton stability as possible rebinding sites become unavailable.

Chains and Loops. Context for these motifs' behavior is provided by replacing all-to-all symmetry with the weaker requirement of translational symmetry. This allows us to consider periodic 1D chains formed of n receptor sites. Here, a transfer matrix can be used to solve for $\Gamma_{\rm off}$ exactly, for any n, so long as primary and secondary sites are equivalent (Supplemental Material, Sec. 6 [28]).

For decreasing *odd* values of n, we see behavior that increasingly reflects the many-to-one case [Fig. 2(a), red]. We may understand this as arising from an increasing frustration

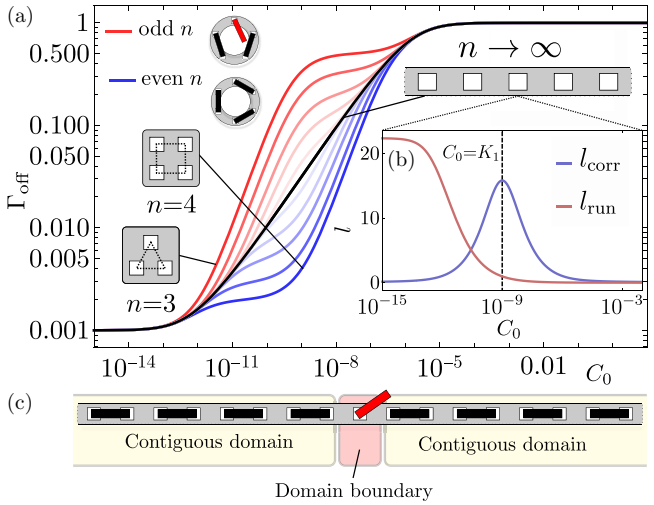

FIG. 2. Frustrated tiling facilitates multi-site exchange. Dissociation rates for odd and even loops of length n differ markedly (panel a). Lighter shades indicate higher values, with $n = 3, 5, 9, 15, 29$ (red) and $n = 4, 6, 10, 16, 30$ (blue). Both odd and even loops converge on the black line [cf. $\Gamma_{\rm off}^{n\to\infty}$ main text] as $n \to \infty$, where many body coordination outweighs frustration due to parity. Run length (approximate) and correlation length (exact) in the $(n \to \infty)$ 1D chain (panel b, inset). Spontaneous dislocations or "domain boundaries" provide sites for multi-site exchange (panel c).

experienced by a baton which cannot reach a more favourable state due to the inability for bivalent molecules to perfectly tile, thus leaving at least one singly bound baton which can participate in multi-site exchange.

By contrast, for decreasing *even* n, multi-site effects are increasingly arrested as the likelihood of perfectly tiling increases [Fig. 2(a), blue], until it reflects the $n_1 = n_2 = 2$ motif for $n = 4$.

In the $n \to \infty$ limit, finite size effects decay away such that the parity of n becomes irrelevant [Fig. 2(a), black], with the role of multi-site exchange being entirely controlled by many-body co-ordination along the lattice, and with binding energetics of individual batons giving way to entropic contributions of combinations. Even though it is favourable for all batons, individually, to be in a perfectly tiled state (such that multi-site effects are absent) the lack of perfect coordination over long distances leads to "domain boundaries"—where contiguous tilings of batons are offset by a single receptor site—allowing locations for multi-site exchange to occur [Fig. 2(c)]. This results in a response to concentration which interpolates between the two extremal behaviors of the all-to-all motifs (Supplemental Material, Sec. 6 [28]) $\Gamma_{\rm off}^{n\to\infty} = 2C_0K_1k_1^{\rm on}/(C_0 - K_1 + \eta)$, where $\eta = \sqrt{(C_0 + K_1)^2 + 4C_0C_{\rm eff}}$.

The characteristic length (in units "sites") of such domains of contiguous doubly-bound batons obeys $l_{\rm corr}^{-1} = \ln[(\eta + C_0 + K_1)/(\eta - C_0 - K_1)]$, which is valid for equivalent primary and secondary sites (Fig. 2(b) and Supplemental Material, Sec. 2 [28]). This vanishes as $C_0 \to 0$ and $C_0 \to \infty$, where cross binding is absent and each site is independent, and peaks at $C_0 = K_1$ where the system most closely achieves a perfect tiling of cross bound molecules. For the parameters used in Fig. 2, the maximum value is $l_{\rm corr} \sim 15$, implying that chains of length $n \gg 15$ are well characterized by the $n \to \infty$ case. More generally, the notion of receptor motifs with (site) translational invariance—i.e., where sites of each type are indistinguishable from each other—allows for a broader class of systems with nontrivial many-body effects. For example, once captured, batons can perform a form of diffusive transport (by "walking") that bears resemblance to both lattice exclusion processes [32,33] and stochastic processes with resetting [34–37], since molecules not only interact with each other through physical occlusion, preventing forward motion, but also compete over receptor sites, thus increasing the likelihood of return to the bulk when they do interact.

One can approximate the mean run length of such motion, implying the existence of a designed, concentration-dependent diffusion constant along the chain. Using a simple combination of the mean life time of a baton and the conditional probability that a neighbor of a given baton is vacant, yields

$$l_{\rm run}^2 \simeq \frac{K_1C_{\rm eff}(C_0 - K_1 + \eta)}{C_0[2K_1(2C_{\rm eff} + K_1) + (C_{\rm eff} + K_1)(C_0 - K_1 + \eta)]}, \quad (1)$$

(Fig. 2(b) and Supplemental Material, Sec. 6 [28]).

Lattices. A further extension is to systems of receptor sites with translational symmetry in 2D, which we treat in the large size limit. Here, the description in terms of integers n_1 and n_2 is retained through the interleaving of lattices of primary and secondary sites such that the they become coordination numbers—i.e., all primary sites have n_2 secondary site neighbors at the baton binding distance, and *vice versa* [Fig. 3(a)]. This description subsumes the one dimensional system (in the limit $n \to \infty$), realized through the choice $n_1 = n_2 = 2$, whilst coordination numbers as high as $n_1 = n_2 = 6$ are possible if the primary/secondary binding sites are indistinguishable. Setting either n_1 or n_2 to one replicates a one-to-many motif.

Exact solutions for lattices with arbitrary coordination numbers are challenging. However, we may construct an approximate solution using short range estimates akin to the cavity method [38]. The approach is detailed in the Supplemental Material, Sec. 7 [28], but consists of calculating conditional occupation probabilities at a distance of one lattice spacing, whilst neglecting higher order correlations. The central quantity required for computing the kinetics is the expected number of doubly bound batons per $n_1 + n_2$ receptor sites, $\mathbb{E}[N_c]$. By defining parameters

$$\gamma = \frac{n_1n_2\big(C_0(C_{\rm eff}(n_1 + n_2) + K_1 + K_2) + C_0^2 + K_1K_2\big)}{2C_{\rm eff}C_0n_1n_2 + 2(C_0 + K_1)(C_0 + K_2)}, \quad (2)$$

$$\beta = \frac{C_0C_{\rm eff}n_1^2n_2^2}{(C_0 + K_1)(C_0 + K_2) + C_0C_{\rm eff}n_1n_2}, \quad (3)$$

this can be expressed as $\mathbb{E}[N_c] = \gamma - \sqrt{\gamma^2 - \beta}$ which can be converted to a probability of a site being occupied by a doubly bound baton, $P(C) = 2\mathbb{E}[N_c]/(n_1 + n_2)$.

For the parameters used in Figs. 1 and 2, this has excellent agreement with simulation, as shown in Fig. 3(b). Moreover, such a result is *exact* for both the $n_1 > 1$, $n_2 = 1$ all-to-all motif, and for infinite 1D chains where loops are absent (and hence, also Bethe lattices [39]).

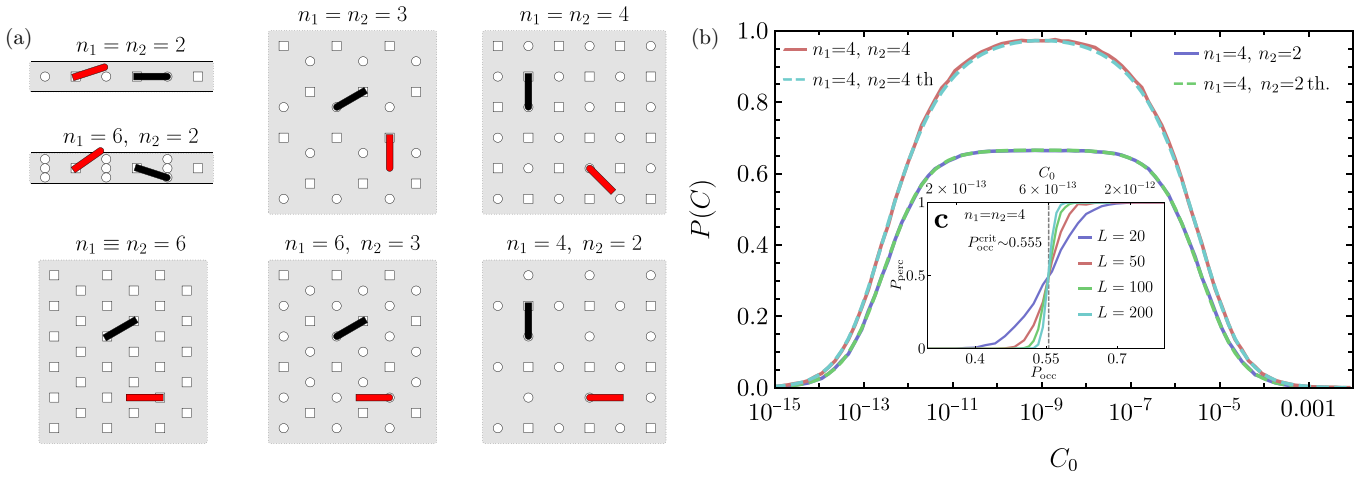

FIG. 3. Translationally invariant 2D lattices with conumbers n_1 and n_2 (panel a): $n_1 = n_2 = 2$ generalizes the $n \to \infty$ 1D chain; $n_1 = 2$, $n_2 = 6$ requires the baton to bind over a (modest) range of distances, and; $n_1 = n_2 = 6$ is only valid for equivalent receptor sites. A cavitylike approximation ($\mathbb{E}[n_c]$, main text, and dashed curves, panel b) agrees with simulation (solid curves, panel b—Supplemental Material, Sec. 7 [28] and [31]) and retains the distinction between equal and unequal coordination numbers seen with both motifs and chains/loops. Probability of a percolating cluster against site occupancy and bulk concentration for the $n_1 = n_2 = 4$ lattice where $n = L^2$ (panel c). The critical probability $P_{\rm occ}^{\rm crit} \simeq 0.555$, is below the conventional site percolation threshold $P_{\rm occ}^{\rm crit} \simeq 0.593$.

Qualitatively, the kinetics follows the principles discerned for 1D loops, indicating the universality of the overarching design principle: equal coordination numbers allow for perfect tiling and are thus more stable, though still subject to a degree of multi-site exchange due to a lack of long range coordination, whilst unequal co-ordination numbers introduce frustration and thus rapid destabilization at low concentrations, despite the infinite lattice.

Many quantitative features of the kinetics, however, depend upon the precise coordination numbers. For instance, the dissociation rate at $C_0 = 0$ is given by $\Gamma_{\rm off}^{C_0=0} = k_1^{\rm on} K_1 K_2 (n_1 + k_r n_2)/(K_2 n_1 + K_1 n_2 + C_{\rm eff} n_1 n_2)$, allowing much higher stability to be realised on lattices where both $n_1 > 1$ and $n_2 > 1$ due to the excess of available receptor sites to all partially bound batons. Other quantitative behaviors involve characteristic destabilization concentrations which depend, to leading order in ε, on the largest coordination number, and timescales of intermediate regimes which depend upon their ratio, both of which are detailed in the Supplemental Material, Sec. 7 [28].

Moreover, the role of bivalency and coordination number extends beyond tunable kinetics to other many body phenomena. For example, such 2D lattices support a percolation transition, for which bivalency changes the critical threshold relative to both conventional monomers and the related (but not identical) case of pure dimers [40–46], which has no singly bound state or exchange phenomenon. On the square lattice ($n_1 = n_2 = 4$) we find the threshold to lie between an estimated lower limit of $P_{\rm occ} \simeq 0.555$ for $K_1 \ll C_{\rm eff}$ [valid for Fig. 3(c)] and the standard result for site percolation with monomers when $C_{\rm eff} \to 0$ ($P_{\rm occ} \simeq 0.593$) [47], with this lower limit lying below the result for pure dimers, $P_{\rm occ} \simeq 0.5619$ [45]. Notably, the control parameter for the transition is the bulk concentration, with critical concentration given by $C_0^{\rm crit} = (4 - P_{\rm crit}) P_{\rm crit} K_1^2/(16(1 - P_{\rm crit})^2 C_{\rm eff}) + \mathcal{O}(\varepsilon^2)$ (Supplemental Material, Sec. 7 [28]). Therefore, as the transition is approached from below, the diverging correlation length is associated with an *increasing* degree of competitive exchange. The implications for the dynamics of the connected domains remains an open question.

Discussion. Arguing that multivalency is best interpreted in the context of classical many-body coordination, we have two main results.

First, the concentration dependence of bivalent kinetics, resulting from spatial patterning, can be understood in terms of an overarching heuristic that encompasses all practical receptor site configurations. This hinges on the notion of geometrical frustration: the extent to which a given configuration cannot be perfectly tiled by batons. When perfect tiling is possible (e.g., equal coordination numbers) substantive multi-site exchange arises from entropic effects only, and is increasingly subdued as system sizes decrease. High levels of frustration (e.g., unequal coordination numbers), by contrast, permit significant multi-site exchange.

Second, our calculations highlight a fact that has been "hiding in plain sight": bivalency is tantamount to a short range interaction, and hence, its effects are synonymous with a variety of emergent spatio-temporal phenomena that rely on many-body coordination. We choose to focus on correlation lengths, mean squared displacements, and percolation, since they allow us to make contact with existing analytical techniques from classical statistical physics. However, there are undoubtedly more exotic features that might be realized by considering higher order multivalency, or receptor sites patterns that vary in either space or time, for example.

We posit that the presented ideas will be relevant to subcellular scale complexes and molecular machines in biology which, rather than being fixed structures, continually exchange their constituent proteins with the bulk, potentially impacting (and/or facilitating new) function [48]. Many of these structures have highly specific symmetries/structures related to their function, suggesting that understanding the role of receptor geometry is essential to comprehending their full behavior. For example, the competitive exchange of different multivalent DNA polymerase subunits which attach to

the six-fold symmetric helicase of the *Escherichia coli* DNA replisome has already been linked with notions of replication speed and DNA lesion repair [11,49]. We therefore speculate that the spatio-temporal features associated with closed loops of receptor sites, including correlation lengths, domain boundaries, and the importance of parity, may be relevant for large complexes with rotational symmetry and/or symmetry mismatches, such as the bacterial flagellar motor [50–53] and nuclear pore complex [54–56].

More generally, and in the context of recent advances in nanoengineering [25], we believe that our work paves the way for a wide range of putative soft systems whose kinetics and emergent spatio-temporal properties might not only be tunable, but designed *a priori* in a rational way.

Acknowledgment. R.E.S. and R.G.M. acknowledge funding from EMBL Australia. The authors thank James Brown, Rokiah Alford, and Jon Berengut for stimulating discussions.

[1] D. J. Diestler and E. W. Knapp, Statistical Thermodynamics of the Stability of Multivalent Ligand-Receptor Complexes, Phys. Rev. Lett. **100**, 178101 (2008).

[2] G. Ercolani and L. Schiaffino, Allosteric, Chelate, and interannular cooperativity: A mise au point, Angew. Chem., Int. Ed. **50**, 1762 (2011).

[3] M. Weber, A. Bujotzek, and R. Haag, Quantifying the rebinding effect in multivalent chemical ligand-receptor systems, J. Chem. Phys. **137**, 054111 (2012).

[4] W. P. Jencks, On the attribution and additivity of binding energies, Proc. Natl. Acad. Sci. USA **78**, 4046 (1981).

[5] S. Erlendsson and K. Teilum, Binding Revisited—Avidity in cellular function and signaling, Front. Mol. Biosci. **7**, 615565 (2021).

[6] R. S. Kane, Thermodynamics of multivalent interactions: Influence of the linker, Langmuir **26**, 8636 (2010).

[7] D. Yu. Zhang and E. Winfree, Control of DNA strand displacement kinetics using toehold exchange, J. Am. Chem. Soc. **131**, 17303 (2009).

[8] B. Gibb, L. F. Ye, S. C. Gergoudis, Y. Kwon, H. Niu, P. Sung, and E. C. Greene, Concentration-dependent exchange of replication protein a on single-stranded DNA revealed by single-molecule imaging, PLoS ONE **9**, e87922 (2014).

[9] S. Cocco, J. F. Marko, and R. Monasson, Stochastic Ratchet Mechanisms for Replacement of Proteins Bound to DNA, Phys. Rev. Lett. **112**, 238101 (2014).

[10] C. E. Sing, M. Olvera de la Cruz, and J. F. Marko, Multiple-binding-site mechanism explains concentration-dependent unbinding rates of DNA-binding proteins, Nucl. Acids Res. **42**, 3783 (2014).

[11] C. Åberg, K. E. Duderstadt, and A. M. van Oijen, Stability versus exchange: A paradox in DNA replication, Nucl. Acids Res. **44**, 4846 (2016).

[12] P. Li, S. Banjade, H.-C. Cheng, S. Kim, B. Chen, L. Guo, M. Llaguno, J. V. Hollingsworth, D. S. King, S. F. Banani, P. S. Russo, Q.-X. Jiang, B. T. Nixon, and M. K. Rosen, Phase transitions in the assembly of multivalent signalling proteins, Nature (London) **483**, 336 (2012).

[13] A. Conway, T. Vazin, D. P. Spelke, N. A. Rode, K. E. Healy, R. S. Kane, and D. V. Schaffer, Multivalent ligands control stem cell behaviour in vitro and in vivo, Nat. Nanotechnol. **8**, 831 (2013).

[14] M. R. Ehrenstein and C. A. Notley, The importance of natural IgM: Scavenger, protector and regulator, Nat. Rev. Immunol. **10**, 778 (2010).

[15] P.-S. Huang, S. E. Boyken, and D. Baker, The coming of age of de novo protein design, Nature (London) **537**, 320 (2016).

[16] X. Pan and T. Kortemme, Recent advances in de novo protein design: Principles, methods, and applications, J. Biol. Chem. **296**, 100558 (2021).

[17] E. Mahon and M. Barboiu, Synthetic multivalency for biological applications, Org. Biomol. Chem. **13**, 10590 (2015).

[18] J. Lowensohn, B. Oyarzún, G. Narváez Paliza, B. M. Mognetti, and W. B. Rogers, Linker-Mediated Phase Behavior of DNA-Coated Colloids, Phys. Rev. X **9**, 041054 (2019).

[19] S. Marbach, J. A. Zheng, and M. Holmes-Cerfon, The nanocaterpillar's random walk: Diffusion with ligand–receptor contacts, Soft Matter **18**, 3130 (2022).

[20] X. Xia, H. Hu, M. P. Ciamarra, and R. Ni, Linker-mediated self-assembly of mobile DNA-coated colloids, Sci. Adv. **6**, eaaz6921 (2020).

[21] M. Röttger, T. Domenech, R. van der Weegen, A. Breuillac, R. Nicolaÿ, and L. Leibler, High-performance vitrimers from commodity thermoplastics through dioxaborolane metathesis, Science **356**, 62 (2017).

[22] S. Wu, H. Yang, S. Huang, and Q. Chen, Relationship between reaction kinetics and chain dynamics of vitrimers based on dioxaborolane metathesis, Macromolecules **53**, 1180 (2020).

[23] G.-R. Yi, D. J. Pine, and S. Sacanna, Recent progress on patchy colloids and their self-assembly, J. Phys.: Condens. Matter **25**, 193101 (2013), publisher: IOP Publishing.

[24] E. Bianchi, R. Blaak, and C. N. Likos, Patchy colloids: State of the art and perspectives, Phys. Chem. Chem. Phys. **13**, 6397 (2011).

[25] J. W. P. Brown, R. G. Alford, J. C. Walsh, R. E. Spinney, S. Y. Xu, S. Hertel, J. F. Berengut, L. M. Spenkelink, A. M. van Oijen, T. Böcking, R. G. Morris, and L. K. Lee, Rapid exchange of stably bound protein and DNA cargo on a DNA origami receptor, ACS Nano **16**, 6455 (2022).

[26] R. H. Kramer and J. W. Karpen, Spanning binding sites on allosteric proteins with polymer-linked ligand dimers, Nature (London) **395**, 710 (1998).

[27] W. J. Errington, B. Bruncsics, and C. A. Sarkar, Mechanisms of noncanonical binding dynamics in multivalent protein–protein interactions, Proc. Natl. Acad. Sci. USA **116**, 25659 (2019).

[28] See Supplemental Material at http://link.aps.org/supplemental/10.1103/PhysRevResearch.4.L042028 for detailed descriptions of baton kinetics, all-to-all motifs, and models of chains and lattices.

[29] M. Abramowitz, *Handbook of Mathematical Functions, with Formulas, Graphs, and Mathematical Tables* (Dover Publications, USA, 1974).

[30] F. Olver, D. Lozier, R. Boisvert, and C. Clark, *The NIST Handbook of Mathematical Functions* (Cambridge University Press, New York, NY, 2010).

[31] R. Spinney, TheoryBioSys/BivalentKinetics: BivalentKinetics (v1.0), Zenodo (2022), https://doi.org/10.5281/zenodo.5899736.

[32] B. Derrida, E. Domany, and D. Mukamel, An exact solution of a one-dimensional asymmetric exclusion model with open boundaries, J. Stat. Phys. **69**, 667 (1992).

[33] G. Schütz and E. Domany, Phase transitions in an exactly soluble one-dimensional exclusion process, J. Stat. Phys. **72**, 277 (1993).

[34] M. R. Evans and S. N. Majumdar, Diffusion with Stochastic Resetting, Phys. Rev. Lett. **106**, 160601 (2011).

[35] A. Pal and S. Reuveni, First Passage under Restart, Phys. Rev. Lett. **118**, 030603 (2017).

[36] A. Pal, I. Eliazar, and S. Reuveni, First Passage under Restart with Branching, Phys. Rev. Lett. **122**, 020602 (2019).

[37] M. R. Evans, S. N. Majumdar, and G. Schehr, Stochastic resetting and applications, J. Phys. A: Math. Theor. **53**, 193001 (2020).

[38] M. Mézard and A. Montanari, *Information, Physics, and Computation*, Oxford Graduate Texts (Oxford University Press, Oxford, 2009).

[39] R. J. Baxter, *Exactly Solved Models in Statistical Mechanics* (Academic Press, London, 1982).

[40] V. A. Cherkasova, Y. Y. Tarasevich, N. I. Lebovka, and N. V. Vygornitskii, Percolation of aligned dimers on a square lattice, Eur. Phys. J. B **74**, 205 (2010).

[41] V. Cornette, A. J Ramirez-Pastor, and F. Nieto, Dependence of the percolation threshold on the size of the percolating species, Phys. A: Stat. Mech. Appl. **327**, 71 (2003).

[42] V. Cornette, A. J. Ramirez-Pastor, and F. Nieto, Percolation of polyatomic species on a square lattice, Eur. Phys. J. B **36**, 391 (2003).

[43] W. Lebrecht, P. M. Centres, and A. J. Ramirez-Pastor, Analytical approximation of the site percolation thresholds for monomers and dimers on two-dimensional lattices, Physica A **516**, 133 (2019).

[44] Y. Leroyer and E. Pommiers, Monte Carlo analysis of percolation of line segments on a square lattice, Phys. Rev. B **50**, 2795 (1994).

[45] Y. Yu. Tarasevich, N. I. Lebovka, and V. V. Laptev, Percolation of linear k-mers on a square lattice: From isotropic through partially ordered to completely aligned states, Phys. Rev. E **86**, 061116 (2012).

[46] N. Vandewalle, S. Galam, and M. Kramer, A new universality for random sequential deposition of needles, Eur. Phys. J. B **14**, 407 (2000).

[47] D. Stauffer and A. Aharony, *Introduction To Percolation Theory: Second Edition*, 2nd ed. (Taylor & Francis, London, 2017).

[48] S. E. Tusk, N. J. Delalez, and R. M. Berry, Subunit Exchange in Protein Complexes, J. Mol. Biol. Plast. Multi-Protein Compl., **430**, 4557 (2018).

[49] C. Indiani, L. D. Langston, O. Yurieva, M. F. Goodman, and M. O'Donnell, Translesion DNA polymerases remodel the replisome and alter the speed of the replicative helicase, Proc. Natl. Acad. Sci. USA **106**, 6031 (2009).

[50] N. J. Delalez, G. H. Wadhams, G. Rosser, Q. Xue, M. T. Brown, I. M. Dobbie, R. M. Berry, M. C. Leake, and J. P. Armitage, Signal-dependent turnover of the bacterial flagellar switch protein FliM, Proc. Natl. Acad. Sci. USA **107**, 11347 (2010).

[51] N. J. Delalez, R. M. Berry, and J. P. Armitage, Stoichiometry and Turnover of the Bacterial Flagellar Switch Protein FliN, mBio **5**, e01216–14.

[52] J. Yuan, R. W. Branch, B. G. Hosu, and H. C. Berg, Adaptation at the output of the chemotaxis signalling pathway, Nature (London) **484**, 233 (2012).

[53] P. P. Lele, B. G. Hosu, and H. C. Berg, Dynamics of mechanosensing in the bacterial flagellar motor, Proc. Natl. Acad. Sci. USA **110**, 11839 (2013).

[54] G. Rabut, V. Doye, and J. Ellenberg, Mapping the dynamic organization of the nuclear pore complex inside single living cells, Nat. Cell. Biol. **6**, 1114 (2004).

[55] K. E. Knockenhauer and T. U. Schwartz, The nuclear pore complex as a flexible and dynamic gate, Cell **164**, 1162 (2016).

[56] Z. Hakhverdyan, K. R. Molloy, S. Keegan, T. Herricks, D. M. Lepore, M. Munson, R. I. Subbotin, D. Fenyö, J. D. Aitchison, J. Fernandez-Martinez, B. T. Chait, and M. P. Rout, Dissecting the structural dynamics of the nuclear pore complex, Mol. Cell **81**, 153 (2021).